Article

Neuron

OLMα2 Cells Bidirectionally Modulate Learning

Highlights

- OLM cells of the intermediate hippocampus express the nicotinic receptor α2 subunit
- Activation of intermediate OLMα2 cells impairs object and fear-related memory encoding
- Inhibition of intermediate OLMα2 cells enhances object memory encoding
- Dorsal and intermediate OLM cells differentially modulate learning

Authors

Samer Siwani, Arthur S.C. França, Sanja Mikulovic, ..., Richardson N. Leão, Adriano B.L. Tort, Klas Kullander

Correspondence

klas.kullander@neuro.uu.se

In Brief

OLM cells have been previously shown to gate information flow into CA1 *in vitro*. Siwani et al. now show that OLM cells of the intermediate hippocampus can either enhance (upon inhibition) or impair (upon activation) memory encoding in freely moving mice.

Siwani et al., 2018, Neuron *99*, 1–9
July 25, 2018
https://doi.org/10.1016/j.neuron.2018.06.022

CellPress

Please cite this article in press as: Siwani et al., OLMα2 Cells Bidirectionally Modulate Learning, Neuron (2018), https://doi.org/10.1016/j.neuron.2018.06.022

Neuron
Article

CellPress

OLMα2 Cells Bidirectionally Modulate Learning

Samer Siwani,[1,3] Arthur S.C. França,[1,2,3,4] Sanja Mikulovic,[1] Amilcar Reis,[1] Markus M. Hilscher,[1,2] Steven J. Edwards,[1] Richardson N. Leão,[1,2] Adriano B.L. Tort,[2] and Klas Kullander[1,5,*]
[1]Developmental Genetics, Department of Neuroscience, Uppsala University, Uppsala 752 37, Uppsala län, Sweden
[2]Brain Institute, Federal University of Rio Grande do Norte, Natal 59056-450, Rio Grande do Norte, Brazil
[3]These authors contributed equally
[4]Current address: Donders Institute for Brain, Behaviour, and Cognition, Nijmegen 6525 EN, Gelderland, Netherlands
[5]Lead contact
*Correspondence: klas.kullander@neuro.uu.se
https://doi.org/10.1016/j.neuron.2018.06.022

SUMMARY

Inhibitory interneurons participate in mnemonic processes. However, defined roles for identified interneuron populations are scarce. A subpopulation of oriens lacunosum-moleculare (OLM) interneurons genetically defined by the expression of the nicotinic receptor α2 subunit has been shown to gate information carried by either the temporoammonic pathway or Schaffer collaterals *in vitro*. Here we set out to determine whether selective modulation of OLMα2 cells in the intermediate CA1 affects learning and memory *in vivo*. Our data show that intermediate OLMα2 cells can either enhance (upon their inhibition) or impair (upon their activation) object memory encoding in freely moving mice, thus exerting bidirectional control. Moreover, we find that OLMα2 cell activation inhibits fear-related memories and that OLMα2 cells respond differently to nicotine in the dorsoventral axis. These results suggest that intermediate OLMα2 cells are an important component in the CA1 microcircuit regulating learning and memory processes.

INTRODUCTION

The hippocampal CA1 area is involved in the recognition of familiar objects (Basu et al., 2016; Rampon et al., 2000) as well as in contextual fear conditioning (Basu et al., 2016; Ji and Maren, 2008; Lee and Kesner, 2004). Pyramidal neurons in CA1 are the last components of the trisynaptic pathway that, together with principal neurons in the dentate gyrus and CA3, forms the major route of information flow through the hippocampus (Andersen, 1975). CA1 pyramidal neurons receive information from within this network via the CA3 Schaffer collaterals and from the entorhinal cortex via the temporoammonic pathway. The mechanisms for memory storage are generally attributed to intrinsic plasticity and long-term potentiation (LTP) at synapses of participating neurons of the network (Benito and Barco, 2010; Daoudal and Debanne, 2003; Martin et al., 2000). A number of studies of hippocampal circuitry have led to the idea that memories generated from entorhinal cortical inputs are influenced by neuromodulators such as acetylcholine (Hasselmo, 1995).

At least 20 different types of inhibitory interneurons with different properties have been described in CA1; some target different portions of the pyramidal cells, whereas others target interneurons (Klausberger and Somogyi, 2008). While interneurons targeting perisomatic domains gate pyramidal cell output, dendritic-targeting interneurons modulate pyramidal cell input (Klausberger and Somogyi, 2008). Among the latter, oriens lacunosum-moleculare (OLM) cells have their soma located in the stratum oriens and send axonal projections to the distal dendrites of pyramidal cells in stratum lacunosum-moleculare, where inputs from the temporoammonic pathway arrive (Leão et al., 2012). OLM cells are thus positioned to control the entrance of multimodal information from the entorhinal cortex into the hippocampus. Notably, OLM cells that specifically express the nicotinic acetylcholine receptor α2 subunit (encoded by the *Chrna2* gene) form a genetically defined population of neurons in the CA1 region of the intermediate hippocampus (OLMα2 cells) (Leão et al., 2012).

Interestingly, OLMα2 cells receive direct cholinergic transmission and respond to nicotine (Leão et al., 2012), and acetylcholine has been implicated in learning and memory processes (Elvander et al., 2004; Tian et al., 2015). Of note, a previous study has shown that inhibition—but not stimulation—of somatostatin-positive cells in the dorsal hippocampus, many of which are OLM cells, prevents fear learning (Lovett-Barron et al., 2014). Nevertheless, since the hippocampus is functionally segregated between the dorsal and the ventral parts (Fanselow and Dong, 2010), it is possible that OLM cells play different roles across the dorsoventral axis. Consistent with this idea, nicotine has opposite effects in the dorsal and ventral hippocampus: while nicotine administration in the dorsal hippocampus enhances contextual fear memory, administration in the ventral hippocampus impairs it (Kenney et al., 2012).

In the present work, we sought to further investigate the role of OLM cells in memory processes. To that end, we activated or silenced OLMα2 cells in the intermediate hippocampus in freely moving *Chrna2-cre* mice in the novel object recognition and contextual passive avoidance tasks.

RESULTS

To study the role of OLMα2 cells in learning, we crossbred *Chrna2-cre* with tdTomato reporter mice to visualize red fluorescent *Chrna2-cre*-expressing cells in the hippocampus (Figure 1). Corroborating our previous study (Leão et al., 2012), the tomato protein was specifically expressed in OLM cells—that is, interneurons with their soma in *stratum oriens* and massive projections to *stratum lacunosum-moleculare* (Figure 1 and Video S1). We delivered the light-gated proton pump archaeorhodopsin (Arch) or the cation channel channelrhodopsin (ChR2) via bilateral injection of double-floxed, inverted, open-reading-frame, adeno-associated viral vectors (Figures 1A and 1B). Since it was previously shown that OLM cells fire in phase with theta activity *in vivo* (Forro et al., 2015), we chose stimulation at 8 Hz, an average theta frequency. By use of the clarity method (Chung and Deisseroth, 2013), we estimated the number of OLMα2 cells reached on each side to 338 out of a total of 3,124 in the cleared hippocampus based on our measured light power at ~1.5 mW/mm^2 at 1 mm, which should suffice to induce activity (Video S1; Histed and Maunsell, 2014). Successfully infected OLMα2 cells also expressed the virally encoded yellow fluorescent protein (EYFP) (Figure 1A). Post-experiment analysis confirmed the targeted location of viral injections and insertion of the light probe into the intermediate hippocampus (Figure 1). We performed patch-clamp recordings to corroborate that OLMα2 cells became responsive to light. Green light inhibited spiking in OLMα2 cells expressing Arch (Figure 1C), and conversely, rhythmic application of blue light at 8 Hz increased spiking in OLMα2 cells expressing ChR2 (Figure 1H). We examined the expression of the immediate early gene c-Fos following light stimulation of Arch- or ChR2-expressing OLMα2 cells in freely moving animals implanted with optical fibers (Figures 1D–1G and 1I–1K; see STAR Methods). The number of c-Fos immunopositive cells after *in vivo* light stimulation in Arch animals (*Chrna2-cre* mice injected with Arch virus) was significantly lower than in injected control *Chrna2-cre* negative mice (Figure 1G). The number of cells in the *stratum oriens* that became immunopositive for c-Fos after *in vivo* light stimulation in ChR2 animals (*Chrna2-cre* mice injected with ChR2 virus) was significantly higher than in control mice (Figure 1K). These results demonstrate that optogenetic tools can control OLMα2 cell activity in freely moving animals.

The recognition of novel objects constitutes a test of episodic-like memory and is impaired in rodents with hippocampal lesions (Antunes and Biala, 2012; Blaser and Heyser, 2015). We next tested whether OLMα2 cells play a role in a novel object recognition task in which animals explored two different objects during 10 minutes in two sessions, named training and test sessions. We first subjected mice to experimental protocols in which—in the training session—a computer coupled to a detection system delivered blue light to both hippocampi of control and ChR2 animals during exploration of one of the two objects (lit object) but not during exploration of the other object (non-lit; Video S2). In the test session performed 24 hr later, the mice were re-exposed to one familiar and one new object. In the protocol named "non-lit object replaced," animals were exposed to the previously lit object and a new object in the test session. Control animals spent more time exploring the new object than ChR2 animals, who explored the new and the previously lit object equally (Figure 2A; Tables S1 and S2), indicating impairment in object recognition. In a control experiment ("lit object replaced"), animals were exposed to the non-lit object and a new object, i.e. two objects not previously associated with OLMα2 cell modulation. In this protocol, both ChR2 and control animals spent more time exploring the new object, with no difference between groups (Figure 2B; Tables S1 and S2). Thus, light-stimulation of OLMα2 cells during training selectively impaired encoding of memory for the lit object.

Since the length of the intersession interval relates to performance in the object recognition test (Hammond et al., 2004), we next investigated whether activating OLMα2 cells would also impair object recognition with an intersession interval of 1 hr. We found similar results as in the 24-hr protocols: ChR2 animals spent equal time with the new and previously lit object, but they recognized the non-lit object (Figures 2C and 2D; Tables S1 and S2). Having found that acute activation of OLMα2 cells during the training session impaired learning, we wondered whether learning could be improved by instead inhibiting OLMα2 cells. To investigate this possibility, we delivered green light during training to mice whose OLMα2 cells expressed Arch (Arch animals). In the test session with the non-lit object replaced, both Arch and control animals exhibited preference for the new object (Table S2). Remarkably, Arch animals spent significantly more time exploring the new object than the previously lit object as compared to control animals (Figure 2E; Tables S1 and S2). We also noticed a lower variability between individual animals displaying high object discrimination in the Arch group. In contrast, replacing the lit object with a new object did not result in any significant differences between groups, and both control and Arch animals exhibited a preference for the new object (Figure 2F; Table S2). Thus, light inhibition of OLMα2 cells selectively improved discrimination for the lit object. Together, the results show that OLMα2 cells can bidirectionally modulate learning.

Next, we wanted to investigate whether the effect of OLMα2 cell stimulation was due to those cells' direct participation in encoding, and we therefore performed protocols with stimulation out of the encoding phase. Light stimulation of OLMα2 cells after the training session did not produce any measurable differences between ChrR2 animals and controls, with both groups showing the expected exploration preference for the novel object in the test session (Figure 3A; Tables S1 and S2). Next, to examine whether the effect of OLMα2 cell stimulation was directly linked to a specific object and not due to stimulation of a spatial component of the field, we stimulated OLMα2 cells when animals were in the arena while disengaged from object exploration. This had no effect on the object preference in the test session (Figure 3B; Tables S1 and S2). Interestingly, and consistent with our findings above, ChR2 but not control animals explored the lit object significantly more when both the lit and non-lit objects were kept in the test session (Figure 3C; Tables S1 and S2); this suggests that ChR2 animals perceived the previously lit object as a new object. Finally, we tested whether light stimuli

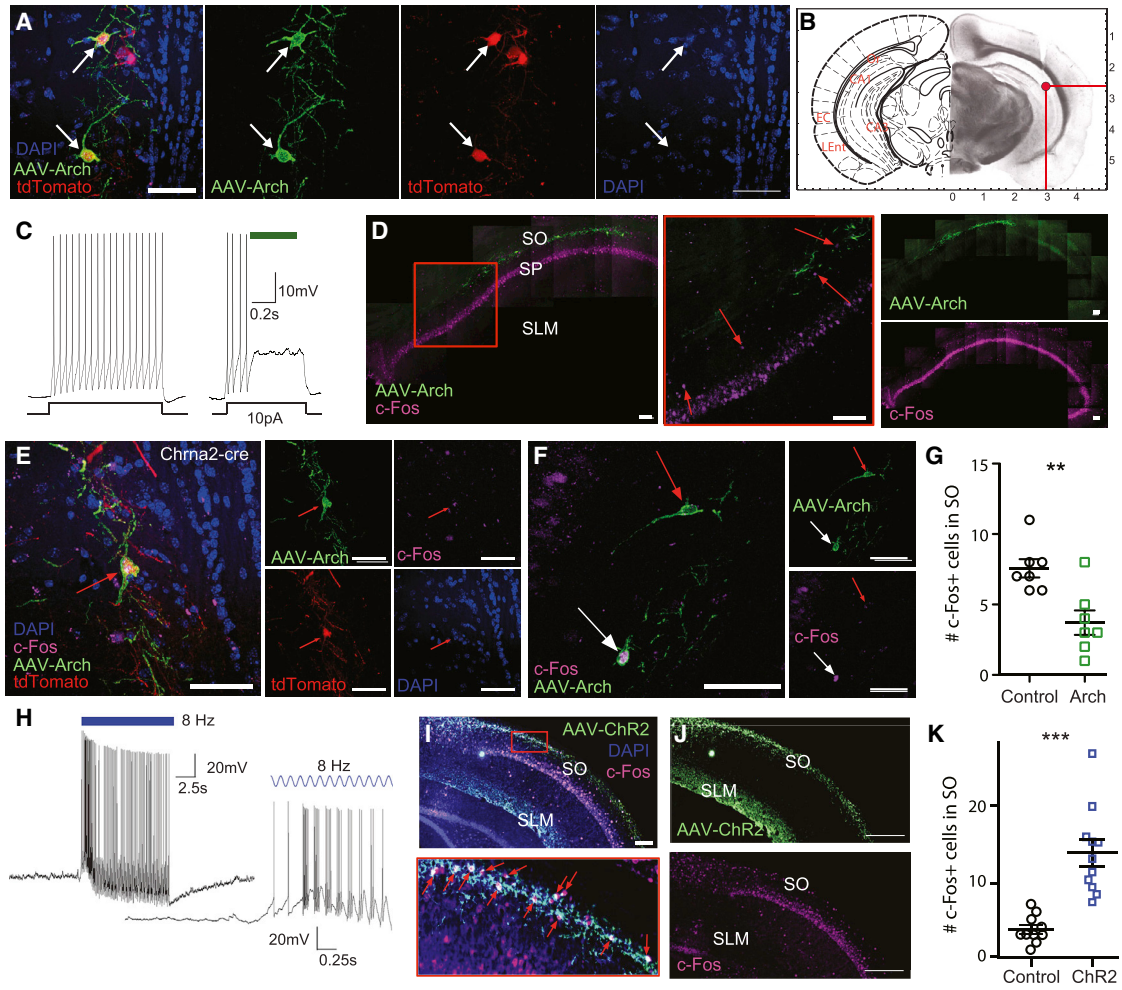

Figure 1. Optical Control of OLMα2 Cell Activity

(A) Confocal image of red OLMα2 cells in an AAV-Arch -injected (green) *Chrna2-cre*/R26tdTomato mouse. Right panels show each marker in separate channels. Notice co-expression of Tomato and Arch in left side (arrows).

(B) Schematic horizontal brain section (left side) and image of a brain slice at the corresponding level (right side) with position of the optical fiber tip marked with a red dot (slice position: interaural 0.72 mm, bregma −3.0 mm). Or; oriens, EC, entorhinal cortex; LEnt; lateral entorhinal cortex, CA1; cornu ammonis 1, CA3; cornu ammonis 3.

(C) Voltage trace from a patch-clamp recording of an OLMα2 cell in a hippocampal slice. Application of green light (green bar) inhibited current-induced spiking in OLMα2 cells from AAV-Arch-injected Chrna2-cre mice.

(D) Microscopy images of hippocampal sections showing green-light-stimulated AAV-Arch-positive OLMα2 cells (green) and c-Fos immunopositive signals (magenta). Left side shows both channels, middle shows enlarged area from red square (arrows point to c-Fos immunopositive signals), and right sides show separate channels.

(E and F) Confocal images of AAV-Arch-positive OLMα2 cells from a *Chrna2-cre*/tdTomato (E) or Chrna2-cre (F) mouse with c-Fos immunostainings. Examples of c-Fos immunopositive (red arrows) and c-Fos immunonegative (white arrows) Arch-infected OLMα2 cells. Right sides show separate channels.

(G) Graph showing number of c-Fos-positive cells in SO after *in vivo* light inhibition for control and Arch groups (mean ± SEM, Arch vs controls, **p<0.01, t test, n = 7 animals/group).

(H) Voltage trace from a patch-clamp recording of an OLMα2 cell in a hippocampal slice. Application of 8-Hz blue light (blue trace) induced spiking in OLMα2 cells from AAV-ChR2-injected *Chrna2-cre* mice.

(I and J) Microscopy images of hippocampal sections showing AAV-Arch-positive OLMα2 cells (green) and c-Fos immunopositive signals (magenta). c-Fos expression was assessed after *in vivo* delivery of blue light to AAV-ChR2-positive OLMα2 cells (green) and c-Fos immunopositive signals (magenta). Arrows in the inset (enlarged area from red square) point to cells co-expressing ChR2 and c-Fos.

(K) Graph showing number of c-Fos-positive cells in SO after *in vivo* light stimulation for control and ChR2 groups (mean ± SEM; ***p < 0.001, t test, n = 11 animals/group). Dapi (blue), tdTomato (red), Arch (green), and c-Fos (magenta). Scale bars, 50 μm.

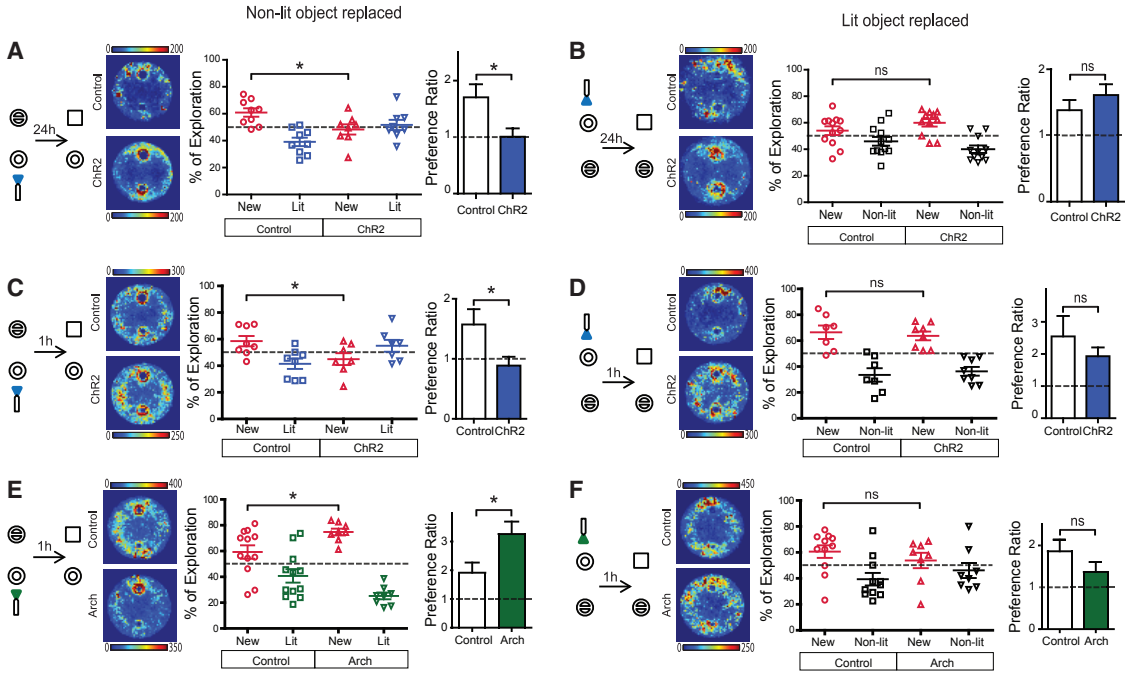

Figure 2. OLMα2 Cells Bidirectionally Control Object Memory Learning

(A–F) Schematic overviews show experimental protocols, heatmaps depict sum spatial occupancy during the test session(s), and graphs show percentage exploration times and preference ratios for the new object. Blue (A–D) or green (E and F) light was selectively delivered during exploration of one of the objects (lit) in the training session. In (A), (C), and (E), the lit object was kept in the test session while the non-lit object was replaced by a new one. In (B), (D), and (F), the lit object was replaced and the non-lit object was kept. ChR2 animals proportionally explored the lit object more than controls (A and C); however, when the lit object was replaced, there was no significant difference between groups (B and D). Conversely, Arch animals proportionally explored the lit object less than controls (E), with no difference between groups when the lit object was replaced (F). The preference ratios were calculated for the new object during the test session. mean ± SEM; *$p < 0.05$, t test.

delivered during both training and test sessions would impact object exploration. Such stimulation protocol did not result in any differences between ChrR2 animals and controls, with both groups showing exploration preference for the novel object in the test session (Figure 3D; Tables S1 and S2).

Rodents depend on the integrity of the hippocampus to produce contextual fear memories (Rudy and Matus-Amat, 2005; Wiltgen et al., 2006). Previous studies have shown that CA1 is involved in contextual fear conditioning (Corcoran et al., 2005; Rudy and Matus-Amat, 2005) and that dorsal somatostatin-positive interneurons play a role in fear learning (Lovett-Barron et al., 2014). We next investigated whether OLMα2 cells may also be involved in the encoding of fear-related memories using a passive inhibitory avoidance task. For this, we used an arena with a brightly lit and a dark compartment (Figure 4A). During training sessions, the animals received a dual foot shock in the dark compartment to acquire an aversion to this normally preferred compartment in future exposures to the arena (test sessions). ChR2 animals that were light-stimulated during training displayed significantly lower latency to enter the dark compartment in the test sessions compared to control animals (Figure 4B; Table S3; Video S3). In contrast, mice whose OLMα2 cells expressed Arch and who were light inhibited during the training sessions showed no difference in latency or velocity compared to controls (Figure 4C; Table S3). Thus, whereas inhibition of OLMα2 cells had no effect, activation of OLMα2 cells impaired aversive memory encoding.

Inhibition of dorsal somatostatin-positive OLM interneurons attenuates fear learning (Lovett-Barron et al., 2014), which is at first glance at odds with our results. Since the test paradigm used in that study differed from the one used here, we modified our protocol and tested the influence of optogenetic modulation to ChR2 and Arch animals in a 5-second period encompassing the foot shock (Figure 4D). For both groups of animals, we did not find any significant differences during training or testing; the re-entry latencies were similar to the control groups (Figures 4E and 4F), suggesting that this type of manipulation onto intermediate OLMα2 cells was insufficient to influence fear learning. It also suggests that activation of intermediate OLMα2 cells could attenuate the memory of the shock when it was paired with the context—i.e,. the chamber—but not when confining OLMα2 cell activation only to the shock event.

This begins to suggest that the dorsal and intermediate part of the CA1 may process encoding and retrieval differently. To further investigate these differences, we repeated the novel object recognition and passive inhibitory avoidance tests with animals that received viral injections and light-mediated inhibition in the dorsal hippocampus ($Arch^{dorsal}$; see STAR Methods). In contrast to the results obtained when inhibiting the intermediate

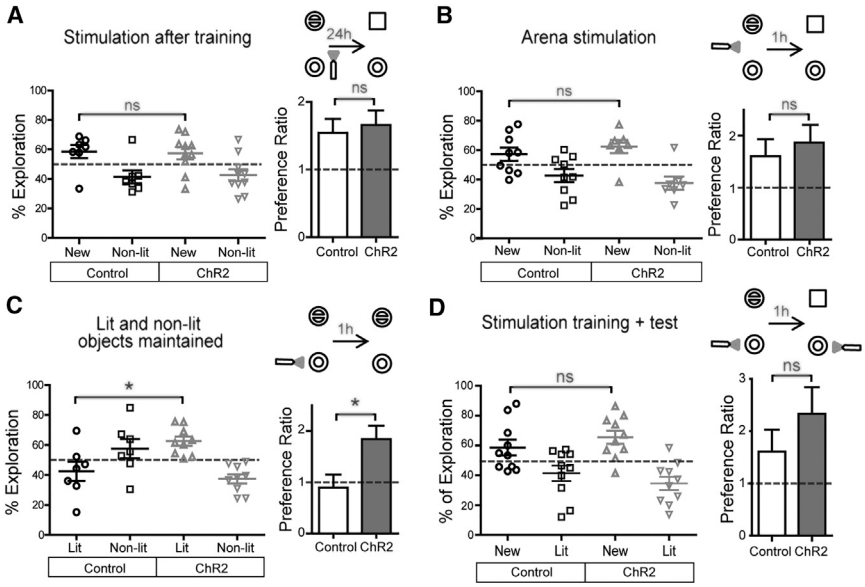

Figure 3. OLMα2 Cells in Object Memory Learning

(A–D) Schematic overviews show experimental protocols and graphs show percentage exploration times and preference ratios. (A and B) Light stimulation after the training session (A), or while animals were not engaged in object exploration (B), led to no difference in object exploration compared to controls. (C) When both objects (lit and non-lit) were kept in the test session, ChR2 mice explored the lit object more, while control animals exhibited no object preference. (D) When light stimuli were delivered also during the test session, the preference for the new object was rescued. The preference ratios were calculated for the new object during the test session (except in C, where preference is calculated for the lit object). Mean ± SEM; *p < 0.05, t test.

CA1 (Figure 2C), we did not find that Arch^{dorsal} animals spent more time exploring the new object than the previously lit object compared to control animals (Figure 5A). However, Arch^{dorsal} animals exhibited lower latency to enter the dark chamber than control groups in the passive inhibitory avoidance task (Figure 5B; Table S3), consistent therefore with the findings of Lovett-Barron et al. (2014) and in contrast to the results obtained for inhibition of OLMα2 cells in the intermediate CA1 (Figure 4C). To gain further insight into the functional differences between the dorsal and intermediate hippocampus, we examined the response of OLMα2 cells to the cholinergic agonist nicotine. In *in vitro* slice experiments, we found that intermediate OLMα2 cells showed a much greater depolarization in response to nicotine than the dorsal counterparts (Figures 5C and 5D), suggesting differential cholinergic influence based on dorsoventral location.

DISCUSSION

Our results suggest that OLMα2 cells in the CA1 region of the intermediate hippocampus can modulate learning of either object or fear-related representations. Acute light-mediated activation of intermediate OLMα2 cells resulted in decreased learning when animals were tested for object recognition as well as fear-related memories. In contrast, light-mediated inhibition improved object recognition but did not affect fear-related memories.

In CA1, the intrahippocampal input from CA3 projects onto proximal apical dendrites of pyramidal cells, whereas the direct external input from the entorhinal cortex contacts the distal apical tuft dendrites (Kajiwara et al., 2008; Takahashi and Magee, 2009). The intrahippocampal indirect pathway is primarily responsible for pattern separation and completion as well as for the association of diverse sets of information, whereas the direct pathway is considered more important for recognizing the novelty of an event or context (Andersen et al., 2006; Lisman and Otmakhova, 2001). Part of the multimodal information necessary for object and context recognition is directly related to the EC-CA1 connections through the temporoammonic pathway. Several hypotheses have been suggested about how this flow of information governs learning and memory. For example, encoding and retrieval are thought to be linked to the theta rhythm such that encoding through external input from the temporoammonic pathway is strong at the peak of theta while Schaffer collateral input is weak (Hasselmo and Stern, 2014; Hasselmo et al., 2002). Vice versa, retrieval would be prioritized in the trough of theta, when synaptic transmission from CA3 is strong. Another influential model posits that the CA1 region would act as a comparator between previously encoded representations in CA3 with current multimodal sensory afferents from the entorhinal cortex, and would thus play a role in novelty detection and act as a trigger for memory formation (Lisman and Grace, 2005; Lisman and Otmakhova, 2001). Anatomical and electrophysiological characterization posits OLMα2 cell activation as a gate switch prioritizing CA3-CA1 inputs over EC-CA1 activity; consistently, LTP induction in the temporoammonic pathway is suppressed when OLMα2 cells are active and enhanced in animals whose OLMα2 cells are non-functional (Leão et al., 2012). Based on this, we hypothesize that, also *in vivo*, inactivation of OLMα2 cells alters circuit dynamics and increases the influence from EC-CA1 input, facilitating encoding of novel environmental input through the temporoammonic pathway and possibly also by concomitant down prioritizing of CA3-CA1 inputs. Likewise, our findings here suggest that acute activation of intermediate OLMα2 cells hinders learning by the opposite mechanism. Combined, our former and present studies contribute to establishing a link between LTP at the cellular level and the behavioral manifestation of a memory.

Acute inhibition of OLMα2 cells improved learning in the object recognition test, but not in the passive inhibitory avoidance test. A reason for this could be that the experience of

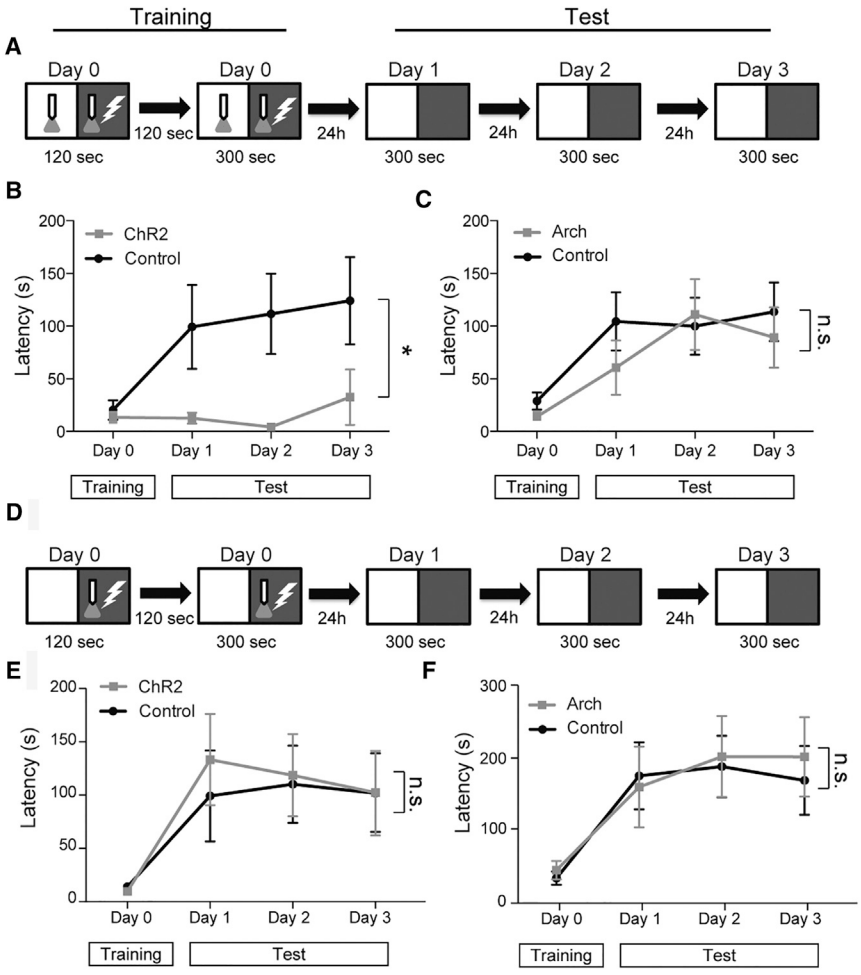

Figure 4. Intermediate OLMα2 Cell Activity Impairs Fear Memory

(A) Task scheme depicting training and test sessions. Light was delivered to the intermediate hippocampus during the training task and was followed by 3 consecutive testing days.

(B and C) ChR2 mice, but not Arch mice, exhibited significantly lower latency to enter in the dark compartment compared with controls.

(D) Task scheme. Light was delivered to the intermediate hippocampus only during the 5-second foot shock.

(E and F) No significant differences were found between the groups in their latency to enter in the dark compartment for either ChR2 or Arch mice compared with their respective controls. Mean ± SEM; *$p < 0.05$ between groups; two-way repeated-measures ANOVA.

the electric shock leads to stronger learning than object exploration and less opportunity for further improvement of encoding. Interestingly, we also found that activation during both encoding and retrieval resulted in normal learning (Figure 3D). A possible reason for this could be that, despite the stimulation of OLMα2 cells during the encoding phase, weak engrams could form, which would be difficult to retrieve. Activation of the same set of OLMα2 cells also during retrieval would facilitate the CA3-CA1 pathway and help recall such weaker engrams. Alternatively, OLM cell activity may influence states and thus participate in state-dependent learning, potentially through an effect on theta rhythms. Another reasonable interpretation—and one in line with the notion of OLMα2 cell activation acting as a gate switch prioritizing CA3-CA1 inputs over EC-CA1 activity (Leão et al., 2012)—is that when OLMα2 cells are light activated, the object memory may be encoded at a different set of synapses, which fail to support recall under baseline conditions. Further studies are needed to establish which of these hypotheses are correct or whether other explanations are at hand.

Our results show that OLMα2 cell activation affected fear-related learning. In the passive inhibitory avoidance test, mice which received intermediate OLMα2 cell activation concomitant with a foot shock maintained similar latencies to enter the dark compartment (shock associated) as in the training day. Control animals increased their latency, thus showing normal aversive memory. A previous study demonstrated that the inactivation of somatostatin-positive interneurons in the oriens layer of the dorsal hippocampus prevents fear learning (Lovett-Barron et al., 2014). We examined whether the different areas of stimulation between the Lovett-Barron et al. (2014) study and our study (dorsal vs. intermediate hippocampus) could underlie the opposite responses. Indeed, we did not observe improved learning in the novel object recognition test when repeating our protocols but instead targeting the dorsal hippocampus (Figures 2C and 5A). Further, we could replicate the results from Lovett-Barron et al. (2014) when we redirected the inhibition of OLMα2 cells to the dorsal hippocampus (Figure 5B). OLMα2 cells are unevenly distributed in the hippocampus, with more cells in the ventral part (Mikulovic et al., 2015), and recent studies have reported on functional subdivisions of the hippocampus along both the transverse and dorsoventral axis (Cembrowski et al., 2016; Ito and Schuman, 2012).

We found here that OLMα2 cells in the intermediate hippocampus were more responsive to nicotine than their dorsal counterparts (Figures 5C and 5D). Interestingly, it has been shown that nicotine administered in the dorsal hippocampus enhances contextual fear memory, while administration in the ventral hippocampus impairs memory (Kenney et al., 2012). Since nicotine activates OLMα2 cells (Leão et al., 2012), this may explain the observed similarity in results when stimulating OLMα2 cells in the intermediate hippocampus (this study) or through inhibition of somatostatin positive

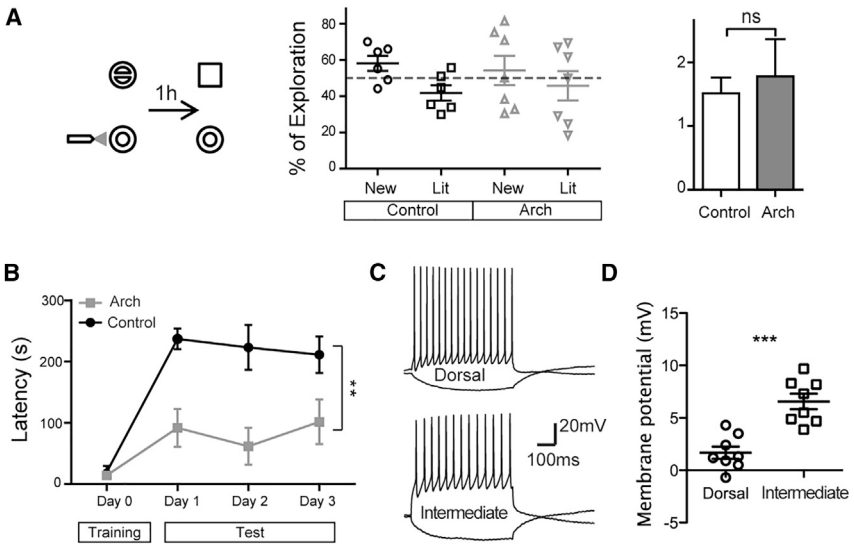

Figure 5. Dorsal OLMα2 Cells Are Functionally Different from Intermediate OLMα2 Cells

(A and B) Same task protocols as in Figures 2E and 4C, respectively, but for light-induced inhibition of dorsal OLMα2 cells. No significant difference was observed in the novel object recognition task (mean ± SEM; $p > 0.05$, t-test). The latency to enter the dark compartment during a passive avoidance task was significantly lower in dorsal-Arch mice than in controls (mean ± SEM ; $^{**}p < 0.01$ between groups; two-way repeated-measures ANOVA).

(C) Examples of current clamp recordings from a dorsal and an intermediate/ventral OLMα2 cell in response to −50 and 100 pA current steps.

(D) Changes in membrane potential of OLMα2 cells caused by nicotine application (1 μM) in the presence of DNQX, dAP5, and picrotoxin. Mean ± SEM; $^{***}p < 0.001$, t test.

cells in the dorsal hippocampus (Lovett-Barron et al., 2014). Acetylcholine can potentiate the Schaffer collateral pathway via activation of nicotinic receptors (Leão et al., 2012; Mann and Greenfield, 2003; Nakauchi et al., 2007); however, other studies have found that this pathway can be inhibited by acetylcholine (Dasari and Gulledge, 2011; Hasselmo and Schnell, 1994; Herreras et al., 1988; Mans et al., 2014; Sheridan and Sutor, 1990). This difference may be due to the timing of incoming inputs or the effect downstream of nicotinic versus metabotropic receptors (Haam and Yakel, 2017). The important role of cholinergic influence from the medial septum for OLM cell activity in learning and memory has recently been demonstrated (Haam et al., 2018). Our findings position intermediate OLM cells in a bidirectional role responding either to inhibitory inputs that improve learning or to excitatory inputs that prevent efficient learning, which possibly is provided by cholinergic action from the medial septum. This is particularly interesting in light of the proposed role for the Chrna2 subunit to provide a molecular switch to continuously excite interneurons of the hippocampus (Jia et al., 2009). It remains to demonstrate whether such a switch is operational in OLM cells in vivo, but if so, this could suggest a mechanism where OLM cells are kept active by the influence from acetylcholine as well as baseline recurrent activation from pyramidal cells. For encoding, the required inactivation of OLM cells could possibly be provided by VIP+ inhibitory interneurons, as has been suggested for Martinotti cells in the neocortex (Pi et al., 2013).

In conclusion, this study provides direct evidence for a role of intermediate OLMα2 cells in memory formation processes, likely through gating of sensory information transmitted from the entorhinal cortex to the hippocampus or from internal processing from Schaffer collaterals. Of note, dysfunctional OLM cell activity has been recently associated with memory deficits in an animal model of Alzheimer's disease (Schmid et al., 2016). Our results suggest that OLMα2 cells can potentially be used as a target for improving learning.

STAR★METHODS

Detailed methods are provided in the online version of this paper and include the following:

- KEY RESOURCES TABLE
- CONTACT FOR REAGENT AND RESOURCE SHARING
- EXPERIMENTAL MODEL AND SUBJECT DETAILS
  - *In vivo* animal studies
- METHOD DETAILS
  - Surgical procedures
  - c-Fos analysis
  - Electrophysiology
  - Habituation
  - Novel object recognition (NOR)
  - Passive inhibitory avoidance
- QUANTIFICATION AND STATISTICAL ANALYSIS
  - Excluded animals
  - Statistical analyses

SUPPLEMENTAL INFORMATION

Supplemental Information includes three tables and three videos and can be found with this article online at https://doi.org/10.1016/j.neuron.2018.06.022.

ACKNOWLEDGEMENTS

We thank George Nascimento for technical support. This work was supported by the Kjell and Märta Beijers Foundation (KDB 943/14), the Swedish Research Council (2015-02395), the Swedish Brain Foundation (FO2013-0139), the Hållsten Foundation (FO2011-0280), The Swedish Foundation for International Cooperation in Research and Higher Education (STINT, BR2017-7095), the Olle Engkvist Byggmästare Foundation (2016/173, S.M.), the Brazilian Federal Agency for Support and Evaluation of Graduate Education (CAPES, 001/12), and the Brazilian National Council of Technological and Scientific Development (CNPq, 306146/2015-0).

AUTHOR CONTRIBUTIONS

A.S.C.F. and S.S. designed and performed the behavior and optogenetic experiments; S.S., A.R., S.M., M.M.H., S.J.E., and R.N.L. performed the c-Fos,

clarity, and ephys experiments; A.B.L.T. and K.K. conceived the study and wrote and edited the final version of the manuscript.

DECLARATION OF INTERESTS

The authors declare no conflicts of interest.

Received: November 22, 2016
Revised: May 17, 2018
Accepted: June 13, 2018
Published: July 5, 2018

REFERENCES

Andersen, P. (1975). Organization of Hippocampal Neurons and Their Interconnections. In: Isaacson, R.L. and Pribram, K.H. (eds) The Hippocampus. Springer. pp. 155–175. 10.1007/978-1-4684-2976-3_7

Andersen, P., Morris, R., Amaral, D., Bliss, T., and O'Keefe, J. (2006). The Hippocampus Book (Oxford University Press).

Antunes, M., and Biala, G. (2012). The novel object recognition memory: neurobiology, test procedure, and its modifications. Cogn. Process. *13*, 93–110.

Basu, J., Zaremba, J.D., Cheung, S.K., Hitti, F.L., Zemelman, B.V., Losonczy, A., and Siegelbaum, S.A. (2016). Gating of hippocampal activity, plasticity, and memory by entorhinal cortex long-range inhibition. Science *351*, aaa5694.

Benito, E., and Barco, A. (2010). CREB's control of intrinsic and synaptic plasticity: implications for CREB-dependent memory models. Trends Neurosci. *33*, 230–240.

Blaser, R., and Heyser, C. (2015). Spontaneous object recognition: a promising approach to the comparative study of memory. Front. Behav. Neurosci. *9*, 183.

Cembrowski, M.S., Bachman, J.L., Wang, L., Sugino, K., Shields, B.C., and Spruston, N. (2016). Spatial Gene-Expression Gradients Underlie Prominent Heterogeneity of CA1 Pyramidal Neurons. Neuron *89*, 351–368.

Chung, K., and Deisseroth, K. (2013). CLARITY for mapping the nervous system. Nat. Methods *10*, 508–513.

Corcoran, K.A., Desmond, T.J., Frey, K.A., and Maren, S. (2005). Hippocampal inactivation disrupts the acquisition and contextual encoding of fear extinction. J. Neurosci. *25*, 8978–8987.

Daoudal, G., and Debanne, D. (2003). Long-term plasticity of intrinsic excitability: learning rules and mechanisms. Learn. Mem. *10*, 456–465.

Dasari, S., and Gulledge, A.T. (2011). M1 and M4 receptors modulate hippocampal pyramidal neurons. J. Neurophysiol. *105*, 779–792.

Elvander, E., Schött, P.A., Sandin, J., Bjelke, B., Kehr, J., Yoshitake, T., and Ögren, S.O. (2004). Intraseptal muscarinic ligands and galanin: influence on hippocampal acetylcholine and cognition. Neuroscience *126*, 541–557.

Fanselow, M.S., and Dong, H.-W. (2010). Are the dorsal and ventral hippocampus functionally distinct structures? Neuron *65*, 7–19.

Forro, T., Valenti, O., Lasztoczi, B., and Klausberger, T. (2015). Temporal organization of GABAergic interneurons in the intermediate CA1 hippocampus during network oscillations. Cereb. Cortex *25*, 1228–1240.

Haam, J., and Yakel, J.L. (2017). Cholinergic modulation of the hippocampal region and memory function. J. Neurochem. *142* (*Suppl 2*), 111–121.

Haam, J., Zhou, J., Cui, G., and Yakel, J.L. (2018). Septal cholinergic neurons gate hippocampal output to entorhinal cortex via oriens lacunosum moleculare interneurons. Proc. Natl. Acad. Sci. USA *115*, E1886–E1895.

Hammond, R.S., Tull, L.E., and Stackman, R.W. (2004). On the delay-dependent involvement of the hippocampus in object recognition memory. Neurobiol. Learn. Mem. *82*, 26–34.

Hasselmo, M.E. (1995). Neuromodulation and cortical function: modeling the physiological basis of behavior. Behav. Brain Res. *67*, 1–27.

Hasselmo, M.E., and Schnell, E. (1994). Laminar selectivity of the cholinergic suppression of synaptic transmission in rat hippocampal region CA1: computational modeling and brain slice physiology. J. Neurosci. *14*, 3898–3914.

Hasselmo, M.E., and Stern, C.E. (2014). Theta rhythm and the encoding and retrieval of space and time. Neuroimage *85*, 656–666.

Hasselmo, M.E., Bodelón, C., and Wyble, B.P. (2002). A proposed function for hippocampal theta rhythm: separate phases of encoding and retrieval enhance reversal of prior learning. Neural Comput. *14*, 793–817.

Herreras, O., Solís, J.M., Herranz, A.S., Martín del Río, R., and Lerma, J. (1988). Sensory modulation of hippocampal transmission. II. Evidence for a cholinergic locus of inhibition in the Schaffer-CA1 synapse. Brain Res. *461*, 303–313.

Histed, M.H., and Maunsell, J.H.R. (2014). Cortical neural populations can guide behavior by integrating inputs linearly, independent of synchrony. Proc. Natl. Acad. Sci. USA *111*, E178–E187.

Ito, H.T., and Schuman, E.M. (2012). Functional division of hippocampal area CA1 via modulatory gating of entorhinal cortical inputs. Hippocampus *22*, 372–387.

Ji, J., and Maren, S. (2008). Differential roles for hippocampal areas CA1 and CA3 in the contextual encoding and retrieval of extinguished fear. Learn. Mem. *15*, 244–251.

Jia, Y., Yamazaki, Y., Nakauchi, S., and Sumikawa, K. (2009). Alpha2 nicotine receptors function as a molecular switch to continuously excite a subset of interneurons in rat hippocampal circuits. Eur. J. Neurosci. *29*, 1588–1603.

Kajiwara, R., Wouterlood, F.G., Sah, A., Boekel, A.J., Baks-te Bulte, L.T.G., and Witter, M.P. (2008). Convergence of entorhinal and CA3 inputs onto pyramidal neurons and interneurons in hippocampal area CA1–an anatomical study in the rat. Hippocampus *18*, 266–280.

Kenney, J.W., Raybuck, J.D., and Gould, T.J. (2012). Nicotinic receptors in the dorsal and ventral hippocampus differentially modulate contextual fear conditioning. Hippocampus *22*, 1681–1690.

Klausberger, T., and Somogyi, P. (2008). Neuronal diversity and temporal dynamics: the unity of hippocampal circuit operations. Science *321*, 53–57.

Leão, R.N., Mikulovic, S., Leão, K.E., Munguba, H., Gezelius, H., Enjin, A., Patra, K., Eriksson, A., Loew, L.M., Tort, A.B.L., and Kullander, K. (2012). OLM interneurons differentially modulate CA3 and entorhinal inputs to hippocampal CA1 neurons. Nat. Neurosci. *15*, 1524–1530.

Lee, I., and Kesner, R.P. (2004). Differential contributions of dorsal hippocampal subregions to memory acquisition and retrieval in contextual fear-conditioning. Hippocampus *14*, 301–310.

Lisman, J.E., and Grace, A.A. (2005). The hippocampal-VTA loop: controlling the entry of information into long-term memory. Neuron *46*, 703–713.

Lisman, J.E., and Otmakhova, N.A. (2001). Storage, recall, and novelty detection of sequences by the hippocampus: elaborating on the SOCRATIC model to account for normal and aberrant effects of dopamine. Hippocampus *11*, 551–568.

Lovett-Barron, M., Kaifosh, P., Kheirbek, M.A., Danielson, N., Zaremba, J.D., Reardon, T.R., Turi, G.F., Hen, R., Zemelman, B.V., and Losonczy, A. (2014). Dendritic inhibition in the hippocampus supports fear learning. Science *343*, 857–863.

Mann, E.O., and Greenfield, S.A. (2003). Novel modulatory mechanisms revealed by the sustained application of nicotine in the guinea-pig hippocampus in vitro. J. Physiol. *551*, 539–550.

Mans, R.A., Warmus, B.A., Smith, C.C., and McMahon, L.L. (2014). An acetylcholinesterase inhibitor, eserine, induces long-term depression at CA3-CA1 synapses in the hippocampus of adult rats. J. Neurophysiol. *112*, 2388–2397.

Martin, S.J., Grimwood, P.D., and Morris, R.G. (2000). Synaptic plasticity and memory: an evaluation of the hypothesis. Annu. Rev. Neurosci. *23*, 649–711.

Mikulovic, S., Restrepo, C.E., Hilscher, M.M., Kullander, K., and Leão, R.N. (2015). Novel markers for OLM interneurons in the hippocampus. Front. Cell. Neurosci. *9*, 201.

Nakauchi, S., Brennan, R.J., Boulter, J., and Sumikawa, K. (2007). Nicotine gates long-term potentiation in the hippocampal CA1 region via the activation of alpha2* nicotinic ACh receptors. Eur. J. Neurosci. *25*, 2666–2681.

Pi, H.-J., Hangya, B., Kvitsiani, D., Sanders, J.I., Huang, Z.J., and Kepecs, A. (2013). Cortical interneurons that specialize in disinhibitory control. Nature *503*, 521–524.

Preibisch, S., Saalfeld, S., and Tomancak, P. (2009). Globally optimal stitching of tiled 3D microscopic image acquisitions. Bioinformatics *25*, 1463–1465.

Rampon, C., Tang, Y.P., Goodhouse, J., Shimizu, E., Kyin, M., and Tsien, J.Z. (2000). Enrichment induces structural changes and recovery from nonspatial memory deficits in CA1 NMDAR1-knockout mice. Nat. Neurosci. *3*, 238–244.

Rudy, J.W., and Matus-Amat, P. (2005). The ventral hippocampus supports a memory representation of context and contextual fear conditioning: implications for a unitary function of the hippocampus. Behav. Neurosci. *119*, 154–163.

Schmid, L.C., Mittag, M., Poll, S., Steffen, J., Wagner, J., Geis, H.-R., Schwarz, I., Schmidt, B., Schwarz, M.K., Remy, S., and Fuhrmann, M. (2016). Dysfunction of Somatostatin-Positive Interneurons Associated with Memory Deficits in an Alzheimer's Disease Model. Neuron *92*, 114–125.

Sheridan, R.D., and Sutor, B. (1990). Presynaptic M1 muscarinic cholinoceptors mediate inhibition of excitatory synaptic transmission in the hippocampus in vitro. Neurosci. Lett. *108*, 273–278.

Takahashi, H., and Magee, J.C. (2009). Pathway interactions and synaptic plasticity in the dendritic tuft regions of CA1 pyramidal neurons. Neuron *62*, 102–111.

Tian, S., Pan, S., and You, Y. (2015). Nicotine enhances the reconsolidation of novel object recognition memory in rats. Pharmacol. Biochem. Behav. *129*, 14–18.

Wiltgen, B.J., Sanders, M.J., Anagnostaras, S.G., Sage, J.R., and Fanselow, M.S. (2006). Context fear learning in the absence of the hippocampus. J. Neurosci. *26*, 5484–5491.

STAR★METHODS

KEY RESOURCES TABLE

REAGENT or RESOURCE	SOURCE	IDENTIFIER
Antibodies		
Goat anti-cFos	Santa Cruz, California, USA	Lot # A0914
Rabbit anti-GFP	Abcam	ab6556
Alexa fluor 647 donkey anti-goat	Thermofisher Scientific	Cat # A2144
Alexa fluor 488 donkey anti-rabbit	Thermofisher Scientific	Cat # R37118
DAPI	Thermofisher Scientific	Cat # 62248
Prolong Diamond Antifade Mountant with DAPI	Thermofisher Scientific	Cat # P36971
Bacterial and Virus Strains		
rAAV2/9.EF1a-DIO-hChR2(H134R)-EYFP.WPRE.hGH	UNC Vectore core	N/A
rAAV2/EF1a-DIO-hChR2(H134R)-EYFP	UNC Vectore core	N/A
rAAV9/Flex-ArchT-GFP	UNC Vectore core	N/A
Chemicals, Peptides, and Recombinant Proteins		
CNQX	Sigma aldrich	CAS# 115066-14-3
Picrotoxin	Sigma aldrich	CAS# 124-87-8
Nicotine hemisulphate (35% in water)	Sigma aldrich	N1019-100ML
Experimental Models: Organisms/Strains		
Gt(ROSA)26Sortm14(CAG−tdTomato)Hze(R26tom)	Allen Brain Institute	N/A
Chrna2-cre:C57bl6	Uppsala University Transgenic Facility, Leão et al., 2012	N/A
Software and Algorithms		
Ethovision XT	Noldus	Versions 9-11
LabVIEW NXG Full Development System	National instruments	Version 2.1
ImageJ (Fiji)	NIH	N/A
Photoshop and Illustrator	Adobe	CS3
ImageJ stitching plugin	Preibisch et al., 2009	Version 1.2
Other		
Ketalar 10mg/mL and 50 mg/mL	Pfizer/OrionPharma	ATC code: N01AX03
Domitor 1mg/mL	Pfizer/OrionPharma	ATC code: QN05cm91
Fiber optic cannula	Doric Lenses	MFC_200/230-0.37_2.7mm_ZF1.25(G)_FLT
Optical patchcord	Doric Lenses	BFP(2)_200/240/400-0.22_1.5m_FCM-2xZF1.25(FP)

CONTACT FOR REAGENT AND RESOURCE SHARING

Further information and requests for resources and reagents should be directed to and will be fulfilled by the Lead Contact, Klas Kullander (klas.kullander@neuro.uu.se).

EXPERIMENTAL MODEL AND SUBJECT DETAILS

In vivo animal studies

We used 145 heterozygote Chrnα2-*cre* transgenic mice bred with homozygote *tdTomato* reporter mice on a mixed genetic background (Sv129:C57bl6) as described in our previous study (Leão et al., 2012). Males and females (3 to 5 months old) were used as isolated groups; effect of gender was not observed and all animals were kept on a 12-hour light/dark cycle with food and water *ad libitum*. All procedures were approved by Uppsala Animal Ethics Committee, Jordbruksverket (C135/14, C132/13).

METHOD DETAILS

Surgical procedures

We delivered channelrhodopsin (ChR2) or archeorhodopsin (Arch) using adeno-associated viral vectors (rAAV2/9.EF1a-DIO-hChR2(H134R)-EYFP.WPRE.hGH (Figures 1 and 2, 3A-C), rAAV2/EF1a-DIO-hChR2(H134R)-EYFP (Figures 3D and 4), rAAV9/Flex-ArchT-GFP. Virus were bilaterally delivered using a nanofil syringe (World Precision Instruments) and a stereotaxic frame at the following coordinates: Intermediate, -3 mm rostrocaudal; -3 and 3 mm mediolateral; -2.7 and -3.6 mm dorsoventral. Dorsal, -1.7 mm rostrocaudal; -1 and 1 mm mediolateral; -1.5 mm dorsoventral. After virus injection, optical fibers (200 μm diameter) were implanted at the same coordinates at a depth of -2.7 mm and fixed with dental cement. Before the behavior experiments, animals were given three weeks for recovery and viral vector driven expression.

c-Fos analysis

Animals were anesthetized by isoflurane inhalation and thereafter deeply anesthetized with injections of a Ketalar/Domitor mix (Pfizer/OrionPharma, Sollentuna, Sweden). The mice were then perfused transcardially with phosphate buffered saline pH 7.4 (PBS) followed by 4% formaldehyde. Brains were removed and placed in 4% formaldehyde at 4°C overnight. Brains were washed 3x in PBS for 10 min, thereafter placed in a solution of 25% sucrose and allowed to settle overnight. Following this, brains were removed from the sucrose solution and stored at -80°C. For cryostat sections, brains were mounted in Tissue-tech™ (Miami, FL, USA) and placed on dry ice, then cut in coronal sections of 35 μm, mounted on glass slides and stored at -80°C until use. Brain sections on glass slides were thawed at room temperature for 45 min. Slides were washed 4x in PBS for 10 min and blocked for 1 hr with blocking solution (2% donkey serum, 1% BSA, 0.1% Triton X-100, 0.05% Tween 20, 0.01M PBS) (1:10). Primary antibody goat anti-cFos (Santa Cruz, California, USA) was diluted (1:150 or 1:500) in Supermix (200 ml TBS, 0.5 g gelatin, 1 ml Triton X-100, heat up to 60 ° C until gelatin dissolves) and slides were incubated for 72 hours at 4°C. During the last 24 hours, primary antibody rabbit anti-GFP (Abcam, Cambridge, UK) diluted in Supermix (1:1000) was added to the slides. Slides were washed 4x in TBS for 10 min. Secondary antibodies (Thermofisher Scientific, Massachusetts, USA) Alexa fluor 647 donkey anti-goat, Alexa fluor 488 donkey anti-rabbit (1:300 or 1:500) and nuclear marker DAPI (1:100 or 1:1000) were diluted in Supermix, added to the slides and left to incubate for 1.5 hours at room temperature. Finally, slides were washed 4x in TBST (0.01% tween) for 10 min and mounted with mowiol. Images were acquired on a Zeiss LSM 510 Meta confocal microscope, using 10x, 20x, 40x and 63x objectives and laser excitation within suitable wavelengths, and thereafter processed with Photoshop CS3 (Adobe) and imageJ to create merged panoramic images and adjusting input levels and color pallet for uniformity across images. For stitching, a plugin for imageJ was used (Preibisch et al., 2009). Number of c-Fos positive cells was counted along the contour of the SO of multiple biological samples (see Figures 1D and 1I) using ImageJ (NIH). Total number of c-Fos positive cells for control and ChR2 or Arch expressing mice was compared by Student's t-test.

Electrophysiology

Horizontal hippocampal slices (300 μm) were obtained from Chrnα2-cre/R26tdTomato mice carrying ChR2 or Arch. Slices were cut using a vibratome (VT1200, Leica, Microsystems). The slices were transferred to a submerged chamber and maintained in artificial cerebrospinal fluid (aCSF: 126 mM NaCl, 2.5 mM KCl, 1.25 mM NaH_2PO_4, 2 mM $MgCl_2$, 2 mM $CaCl_2$, 26 mM $NaHCO_3$ and 10 mM glucose), constantly bubbled with 95% O_2 and 5% CO_2. Patch pipettes from borosilicate glass capillaries (GC150F-10 Harvard Apparatus) were pulled on a vertical puller (Narishige, Japan) with resistance around 7 MΩ and filled with internal solution containing: 130 mM K-gluconate, 7 mM NaCl, 0.3 mM $MgCl_2$, 2 mM ATP, 0.5 mM GTP, 10 mM HEPES and 0.1 mM EGTA (pH was adjusted to 7.2 using KOH). Current-clamp recordings were obtained using a Multiclamp 700B (Molecular Devices) amplifier. Data was acquired by a National Instruments DAQ card and WinWCP/WinEDR softwares implemented by Dr. J. Dempster (University of Strathclyde, Glasgow, UK). 8-Hz sinusoid function (varying from 0 to 4 mW at the tip of the fiber) drove a 473-nm laser (Shanghai Dream Lasers analog modulated) to activate ChR2 expressing cells. Square light pulses (555-nm laser, Shanghai Dream Lasers) were used to inhibit Arch expressing cells. For experiments testing nicotine sensitivity, membrane potential in free run was measured under the presence of 50uM dAP5, 10uM CNQX and 10uM picrotoxin (Sigma) with or without 1uM Nicotine hemisulphate (Sigma aldrich).

Habituation

Before the behavioral tasks, the animals were handled by the experimenter in 5-minute sessions inside the experimental room for three consecutive days. During these sessions, they were also habituated to mounting of the optic fiber.

Novel object recognition (NOR)

To assess the encoding of object memory, we used six different protocols of the NOR task (listed below). We placed two objects of similar size in a round arena (46 cm diameter; Video S2). During the training session, animals were allowed to explore the arena with the objects for 10 min. The test session was performed either 1 hour or 24 hours apart. In the test session, we replaced one of the objects with a novel one (except in Figure 3C) and once again allowed mice to explore the arena for 10 min. The preference ratio was defined as the time exploring the novel object divided by time exploring the familiar object (except in Figure 3C, where it was defined as the time exploring the lit object divided by the time exploring the non-lit object). Mice were subjected to the following protocols: (1) Non-lit object replaced: during the training session, light was delivered for a minimum of 1 second when the animal approached one

of the objects (lit object), but not the other (non-lit object); light delivery was only turned off when the animal stopped exploring the object (Video S2). In the test session, the non-lit object was replaced by a new object. (2) Lit object replaced: the training session was performed as described above, but in the test session the lit object was replaced by a new object. (3) Arena stimulation: during the training session light was delivered when animals were not engaged in object exploration. During the test session, one of the objects was replaced by a new object. (4) Stimuli after training: no light was delivered during the training session; immediately after training, light was delivered in windows of 10 seconds on and off for 10 minutes. In the test session one of the objects was replaced by a new object. (5) Lit and non-lit objects maintained: the training session was performed as in protocol 1. In the test session, no object was replaced. During the training session, light was delivered. (6) Similar protocol as (1) but with light delivery during both the training and test sessions. During the recording, the experimenter was not present in the behavioral room. Light delivery was automated using a national instruments board (USB-6351) controlled by Ethovision software (XT, versions 9-11) through a custom designed Labview software. Light was delivered bilaterally at theta frequency (8 Hz) with an intensity of ~4 mW. The trigger for light delivery was automatically set as when the animal head entered the "object zone", defined in Ethovision as the distance of 1 cm from the edge of the object. The same animal was not used in more than two different protocols.

Passive inhibitory avoidance

The apparatus consisted of two chambers without roof: one light chamber with white walls (~3200 lux) and one dark chamber with black walls (closed door ~4 lux, open door ~9 lux). The light chamber had two 3-W lamps illuminating the chamber. During training, the animal was placed in the light chamber for 30 seconds. Next, the door connecting the two chambers was opened (see Video S3). When the animal entered the dark chamber, the door was closed and a shock was delivered after 5 seconds (1 mA, 100 ms). These procedures were done manually. The animal was brought to the home cage for two minutes; afterwards, the animal was subjected to another trial in the same arena (same shock amplitude and duration). The maximum latency to enter the dark chamber was 90 seconds for the first trial and 270 seconds for the second trial. Animals that did not exit the light chamber in the training trials were excluded from further analysis. For the data analysis, the latency time to enter in the dark chamber was averaged for the two trials in the training session (day 0). Velocity was measured by Ethovision software when animals were in the light chamber and was averaged for the two trials in the training session (day 0). Latency was automatically measured in one trial for test days 1-3. Two stimulation protocols were used during the training session: (1) light was delivered bilaterally at theta frequency (8 Hz) with an intensity of ~4 mW in periods of 1 second on and 1 second off (to reduce the probability of cell death due to over activation or heatshock) for the whole duration of the task or (2) for 5 continuous seconds starting one second before delivery of the foot shock. We performed three test sessions separated by 24 hours (day 1, day 2 and day 3). In the test session, no shock was delivered and animals were allowed a maximum latency of 270 seconds to enter the dark chamber. Animals that did not exit the light chamber after 270 seconds were placed in the dark chamber for ~10 seconds to have all mice exposed to the pairing of CS - no US before being retested in subsequent days. This procedure was implemented to minimize differences in memory extinction within groups. During recording sessions, the experimenter was present in the behavioral room but not visible to the animal, positioned on the side of the arena between the dark and the light chamber so as to not induce place preference.

QUANTIFICATION AND STATISTICAL ANALYSIS

Excluded animals

In the NOR task, we excluded animals that had the optical fiber unplugged during the training session and animals that explored the objects less than 10 sec (5/145). We also excluded animals in the passive inhibitory avoidance task that did not enter the dark chamber during the training sessions or escaped the chamber (9/109).

Statistical analyses

Tracking data were extracted and scored from video recordings using the Ethovision software (XT, versions 9-11). The normality distribution test (Shapiro-Wilk normality test) was applied to each dataset. We performed t-tests to compare data with Gaussian distribution, otherwise the Mann-Whitney test was used. Data are presented as mean and standard error of the mean (SEM). For the passive inhibitory avoidance task, we performed two-way repeated measures ANOVA using animal group and day as independent variables. Numerical details of all statistical analyses are provided in Tables S1, S2, and S3.